

---

## CHAPTER 8: CONTROLLER DESIGN

### 8.1 INTRODUCTION

In this chapter the basic controller design is done on the simplified linear model. This design is done in the Matlab® environment with the MPC toolbox [12]. This toolbox enables the user to design a controller with various options. The design tools are the cost function weight multipliers, for the inputs and the outputs, the input and output limits and the manipulation and prediction horizons. An increase in the input cost function weights smooth the manipulator signals, while an increase in the output cost function weights forces the outputs closer to their setpoints. The manipulation (M) and prediction (P) horizons affect the optimisation of the cost function. It may appear that controller design with MPC is done by trial and error, but the effects of each parameter can be determined from repeated experiments. The design method will be shown step by step. The controller is tested for the same operating conditions as in Chapters 5 & 6.

In Section 8.2 the properties of Model Predictive Control (MPC) are discussed. Section 8.3 gives the basic design procedure for MPC. Section 8.4 shows the inclusion of an integrator in the controller, and motivates the choice of integral cost function weight.

### 8.2 MODEL PREDICTIVE CONTROL

The control method that was selected for this project is MPC [11]. The MPC strategy results from the optimisation of a performance index with respect to a future control sequence, using predictions of the output signals based on an internal process model. An optimisation algorithm is applied to compute a sequence of future control signals that minimises the performance index subject to the given constraints. MPC uses the receding horizon principle. This means that after computation of the optimal control sequence, only the first control is implemented. The horizon is shifted one time step and the optimisation is repeated with new information of the measurements. Clarke and Scattolini [45] give a discussion of the receding horizon principle.

It is assumed that a proper furnace control system is already in place. This control system uses MVs such as the electric arc current and voltage, the DRI feed-rate and the oxygen injection rate. This dissertation treats those MVs as disturbances. Those MVs that are operator controlled through the furnace control system is regarded as unmeasurable disturbances, since operator control is frequently applied with override mechanisms. Those MVs that are automatically controlled by the furnace controller are regarded as measurable disturbances, since the control system generates their command values and can simultaneously relay those values to any other control system. MPC makes use of the measurement of measured disturbances in its optimisation.

Under certain conditions, the future trajectories for some of the MVs are also known. This leads to the observation that MPC combines feed-forward and feedback control. Feed-forward control is done because MPC can predict undesired behaviour in response to disturbances, and is capable of correcting for such behaviour in advance (for measured disturbances). Feedback control is done in that MPC recalculates each control with the newest measurement of the outputs. For a comparison of the advantages and disadvantages of feed-forward and feedback control see [21].

The use of an internal model makes MPC very attractive. When a very good internal model is available, feed-forward control performs better than feedback control, because it is not affected by process lag and does not introduce instability in the closed loop response. The linearised model is not that good that it can be used in pure feed-forward control, but combined with MPC it will compensate for the lack of measurable data. The use of real-time optimisation also makes MPC attractive. Optimisation enables a controller to control a larger number of controlled variables (CVs) than the number of available manipulated variables (MVs). This is achieved by the selection of cost function weights and limits. While all the CVs are within their specified limits, the cost function is minimised with the ordinary cost function weights. When a CV is predicted to exceed a specified limit, the controller attempts to prevent it by selection of MVs, to obtain feasible optimal control. Therefore, by the optimisation of the cost of internal model predictions, MPC can use two MVs to control three CVs, depending on the feasibility due to the constraints.

For a Generalised Predictive Control [46] performance index (a quadratic cost function), and linear constraints, the solution can be found using quadratic programming algorithms. For this dissertation a quadratic-programming algorithm formulated by G.B. Dantzig is used, as this algorithm displays fast convergence [47]. According to Morari and Ricker [12] MPC displays its main strength when applied to problems with:

- A large number of manipulated and controlled variables;
- Constraints imposed on the manipulated variables;
- Changing control objectives or equipment failures.

Although MPC is in fact a time-variant system (due to real-time optimisation) it is possible to design a much-simplified pre-computed (time-invariant) controller, on the condition that no constraints may be applied. Bordons and Camacho [48] illustrate a practical example of this, where they show that the pre-computed MPC is computationally much less demanding, and can therefore work at a much shorter sampling time than MPC with real-time optimisation (on the same machine). In this system however, the constraints are crucial, since they are actual physical constraints. Thus only MPC with true real-time optimisation will be considered.



## 8.3 CONTROLLER DESIGN

### 8.3.1 Design Tools

The MPC toolbox of Matlab® was used [12]. The toolbox Mod-format is used, and to obtain it, the matrices B&E and D&F are combined. The “A” and “B” matrices are converted to the discrete time format. The internal and plant models are the same, except that the unmeasured disturbances affect the plant, while the internal model is not affected by the unmeasured disturbances. The effects of the unmeasured disturbances are only detected in the measured outputs.

The controller design parameters are the prediction and manipulation horizons and the cost function weights, for outputs and inputs. An increase in the input cost function weights smooth the manipulator signals, while an increase in the output cost function weights forces the outputs closer to their setpoints. The manipulation and prediction horizons affect the optimisation of the cost function. The use of each is shown step by step towards the best controller design. First the initial parameter selection is discussed, and then the changes are shown step by step.

### 8.3.2 Initial parameter selection

The initial output cost function weight selection was based on a semi-normalised cost for the three controlled variables (relative pressure, off-gas temperature, off-gas %CO). The cost function takes the following general form where  $\bar{\gamma} = \bar{r} - \bar{y}$  is the error vector, the difference between the controlled variables and setpoints.

$$\psi(\bar{\gamma}, \bar{u}) = \frac{1}{2} \bar{\gamma}' Y \bar{\gamma} + \frac{1}{2} \bar{u}' U \bar{u} \quad (8-1)$$

The errors for the outputs were approximated as the absolute values of the setpoints or CV limits. For the three controlled variables this translates to  $\gamma_a = [5, 1, 773]$ . A completely normalised output cost weight matrix would then yield  $\text{diag}(Y) = [0.04, 1, 1.67E-6]$ . It was found that this cost function weight selection is completely biased in favour of the off-gas composition.

The off-gas composition is less controllable than either of the other controlled variables, and in addition its linear model estimate is worse than the others are (see Fig.6.10-13). A completely normalised output cost is thus not preferred. Even when the output cost weight matrix elements are simply made equal to the inverse of the corresponding error estimates, the same bias toward the off-gas composition was experienced, which resulted in poor or no control of all three variables at all. The output cost weight matrix elements are therefore made equal to the square root of the corresponding error estimate inverse:  $\text{diag}(Y) = [0.45, 1, 0.036]$ .

The input ranges are approximately the same and the input cost weight matrix is therefore made a unity matrix. The horizons are initially  $M = 1$  and  $P = 2$ , which is a minimum requirement for this system, as  $P=1$  results in an infeasible Quadratic Programming (QP) problem. This minimum requirement is the initial selection, since it results in the smallest computational requirement.

For the design procedure, the output limits will not be applied, since they only make the design procedure more difficult (infeasible QP), while the outputs are not yet satisfactorily controlled. The output limits will only be applied in the plant simulation, which will be demonstrated in the next chapter. For the design procedure, and for all time-domain analysis, the input limits will be applied. In the case where hard constraints are imposed, the resulting control law is generally non-linear. The performance of such a control system has to be evaluated by time-simulation [12]. In the solution of the problem at hand there were important physical constraints as shown in Table 8.1. The rate constraints are expressed as a percentage of the maximum range of the MVs. Due to these constraints the control law had to be evaluated by means of time simulations.

Table 8.1: Constraints on manipulated variables

Fan Power: $u_1$			Slip-gap width: $u_2$		
Min	Rate	Max	Min	Rate	Max
0 MW	1% / s	1 MW	0.1 m	1% / s	0.5 m

Table 8.2 gives a summary of the initial parameter selection ( $Y,U,M,P$ ) and the output reference ( $R$ ) signals. The reference signals for the outputs are chosen lower than the limits (where there are limits, although not applied), in order to prevent “Bang-bang control” in the implementation phase:

Table 8.2: Initial parameter selection summary C8.0

$Y(1)$	$\bar{r}(1)$	$Y(2)$	$\bar{r}(2)$	$Y(3)$	$\bar{r}(3)$	$U(1)$	$U(2)$	$M$	$P$
0.45	-5 Pa	1	0.5 %	0.036	753 K	1	1	1	2

### 8.3.3 Initial controller test

The fan power control signal is shown in Fig.8.1, and the slip-gap in Fig.8.2:

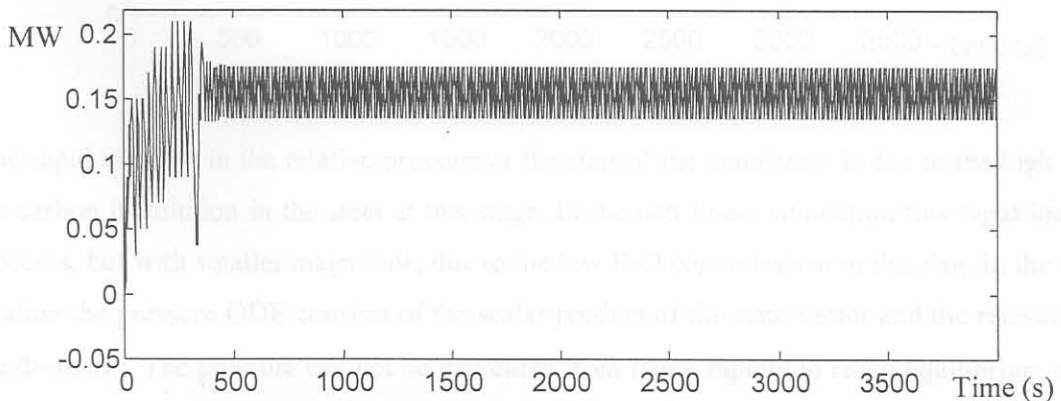


Figure 8.1 Fan power control action (initial controller settings)

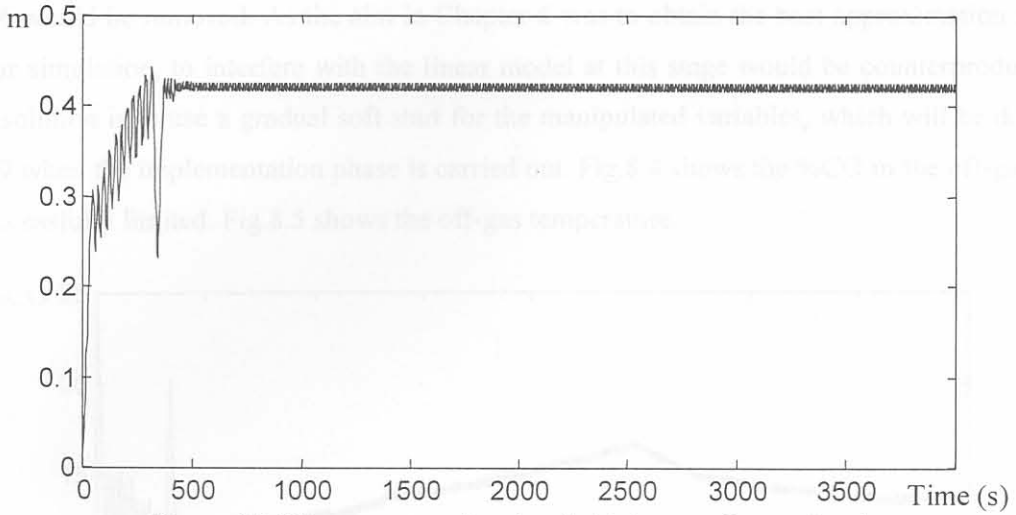


Figure 8.2 Slip-gap control action (initial controller settings)

It is seen from the preceding two figures that both control signals enter a limit cycle, also known as “ringing” [12]. In general this is undesirable in a controller as it adds unnecessary high frequency components that wear out actuators. The time step (sampling time) is one second. The initial controller is not successful as shown in the next three figures. Fig.8.3 shows the relative pressure, which does not even achieve a negative value.

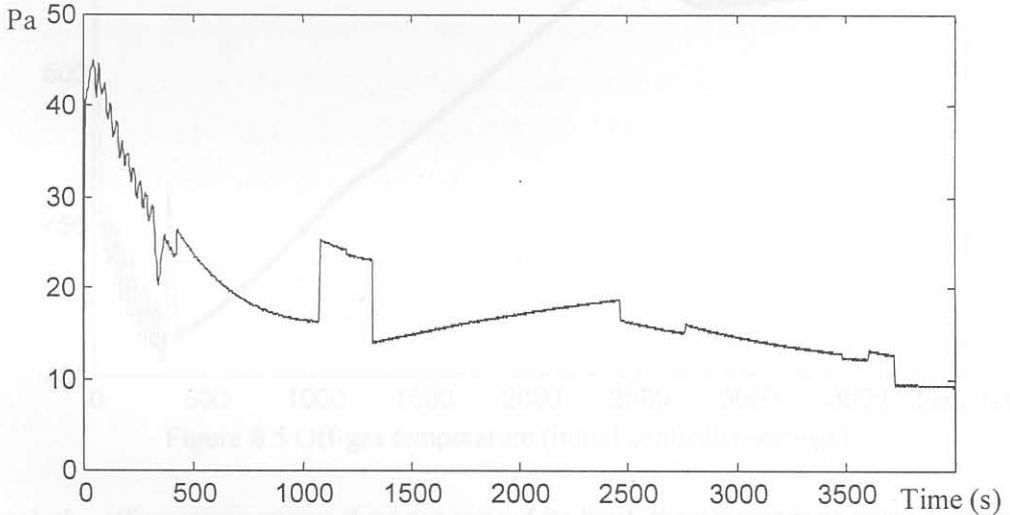


Figure 8.3 Relative pressure (initial controller settings)

The rapid increase in the relative pressure at the start of the simulation is due to the high value of the carbon in solution in the steel at this stage. In the non-linear simulation this rapid increase also occurs, but with smaller magnitude, due to the low FeO concentration in the slag. In the linear simulation the pressure ODE consists of the scalar product of the state vector and the relevant row of the  $\Phi$ -matrix. The pressure can not be prevented from rising rapidly to reach equilibrium due to the ODE. The corresponding elements in the  $\Phi$ -matrix could be removed, but then the aim of



Chapter 6 would be removed. As the aim in Chapter 6 was to obtain the best approximation to the non-linear simulation, to interfere with the linear model at this stage would be counterproductive. Another solution is to use a gradual soft start for the manipulated variables, which will be done in Chapter 9 when the implementation phase is carried out. Fig.8.4 shows the %CO in the off-gas that is not successfully limited. Fig.8.5 shows the off-gas temperature.

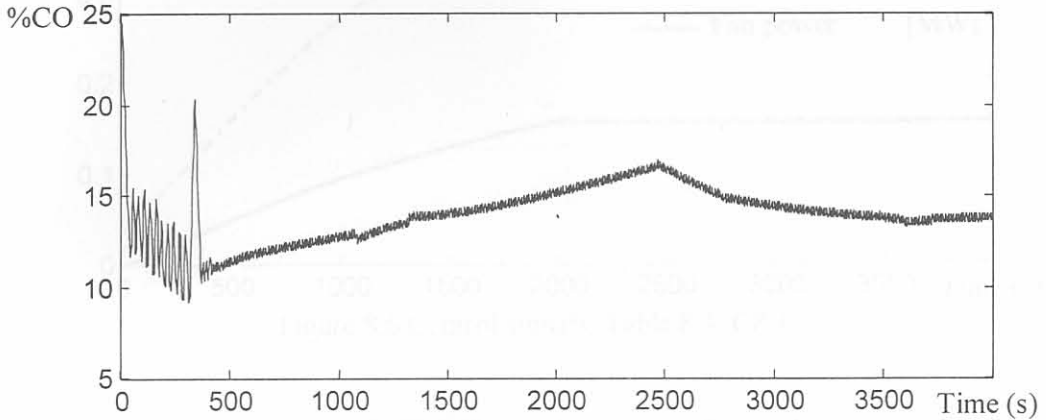


Figure 8.4 %CO in off-gas (initial controller settings)

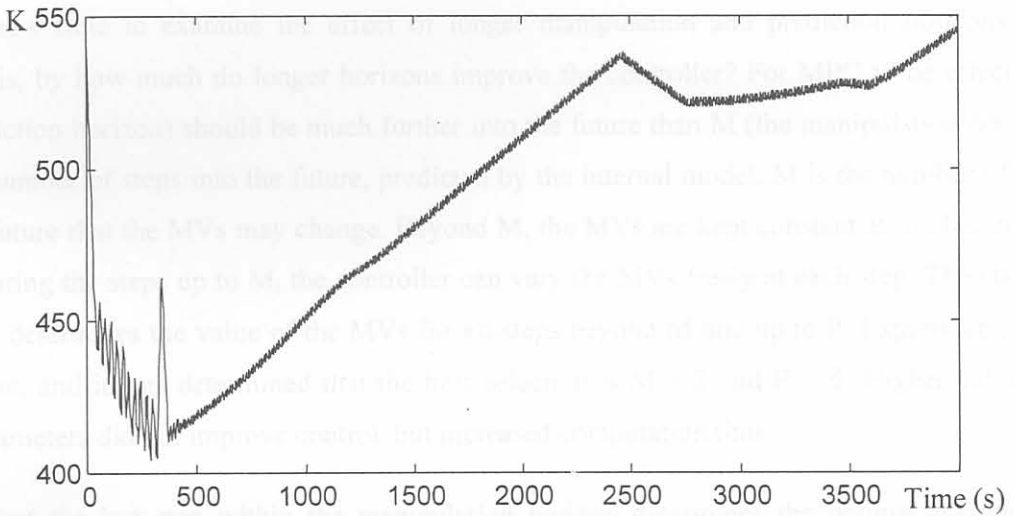


Figure 8.5 Off-gas temperature (initial controller settings)

Although the off-gas temperature does not exceed its limit, the process runs more economically if it is closer to its limit. In conclusion, the initial controller settings yield a noisy, unsuccessful controller. Before an attempt is made to improve the control, the manipulator noise must be reduced. Increasing the input cost weights, in the matrix  $U$  equation (8-1) can achieve this. Experiments were carried out to determine the input cost weight selection. The final result is shown here, with the input cost weights at 400 each. The new controller settings are in Table 8.3:

Table 8.3: Controller settings C8.1

Y(1)	Y(2)	Y(3)	U(1)	U(2)	M	P
0.45	1	0.036	400	400	1	2

The control responses shown in Fig.8.6 are much smoother than those in Fig.8.1 and Fig.8.2.

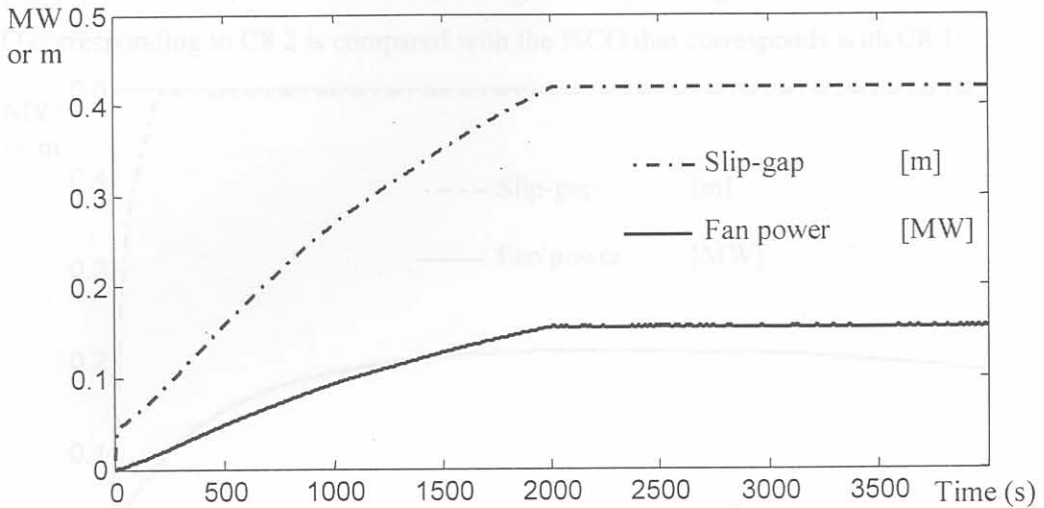


Figure 8.6 Control signals: Table 8.3: C8.1

### 8.3.4 Horizon Selection

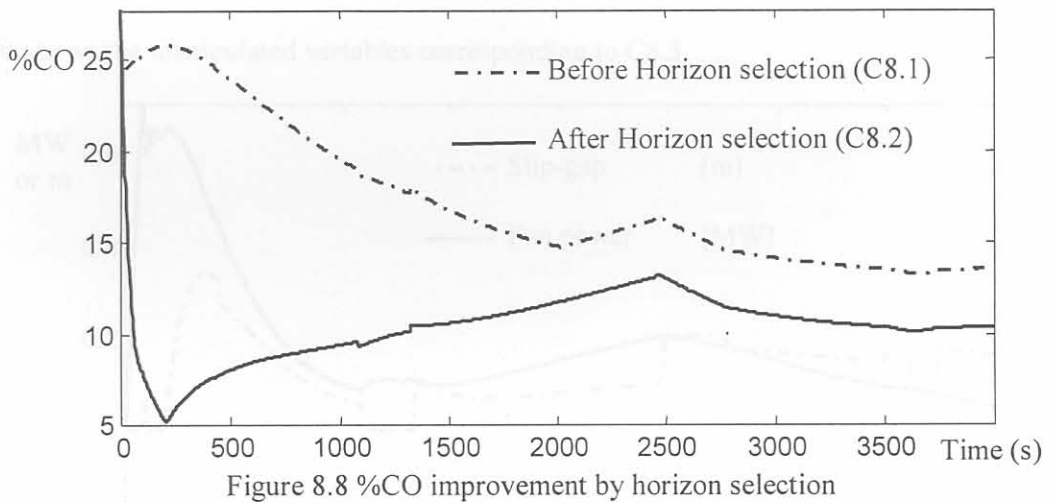
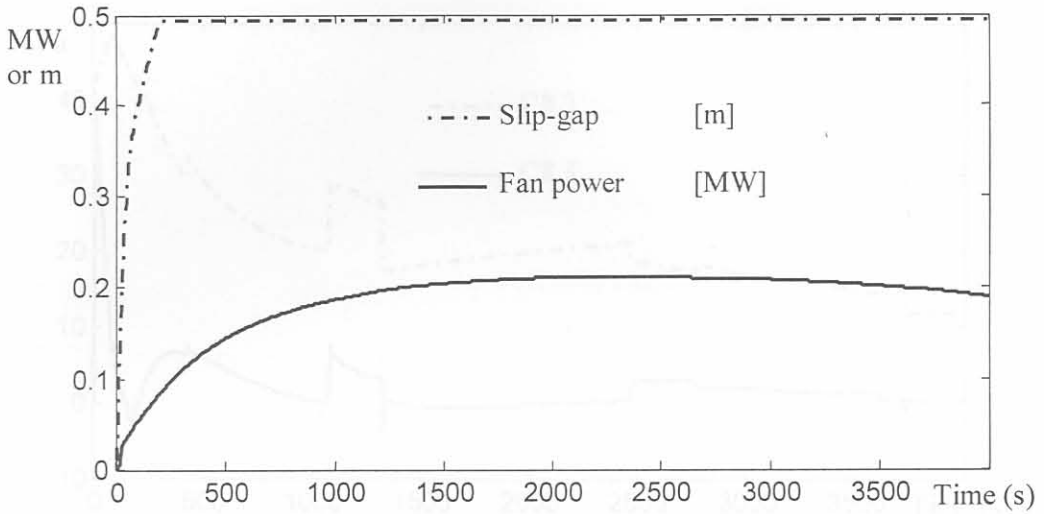
It is now time to examine the effect of longer manipulation and prediction horizons. The question is, by how much do longer horizons improve the controller? For MPC to be effective  $P$  (the prediction horizon) should be much further into the future than  $M$  (the manipulation horizon).  $P$  is the number of steps into the future, predicted by the internal model.  $M$  is the number of steps into the future that the MVs may change. Beyond  $M$ , the MVs are kept constant at the last control value. During the steps up to  $M$ , the controller can vary the MVs freely at each step. The last step before  $M$  determines the value of the MVs for all steps beyond  $M$  and up to  $P$ . Experiments were carried out, and it was determined that the best selection is  $M = 2$  and  $P = 6$ . Higher values for these parameters did not improve control, but increased computation time.

In effect the last step within the manipulation horizon determines the optimal manipulated variables in quasi-steady state. The time duration of this quasi-steady state ( $P-M$ ) should preferably be an order of magnitude larger than  $M$ , to make it an approximation to steady state. Another way to see it is in terms of the dead time of the process response to the manipulated variables. The prediction horizon should extend beyond the manipulation horizon by more than the process dead time [49] (which is 1.09 s for the reaction time plus 1-2 s for the transport delay). If ( $P-M$ ) is shorter than the dead time, the effect of the manipulation changes will not be seen in the prediction. The new controller settings are shown in Table 8.4:

Table 8.4: Controller settings C8.2

Y(1)	Y(2)	Y(3)	U(1)	U(2)	M	P
0.45	1	0.036	400	400	<b>2</b>	<b>6</b>

The control signals for C8.2 are shown in Fig.8.7. The horizon selection mainly caused an improvement in the %CO, which was reduced significantly throughout the simulation. In Fig.8.8 the %CO corresponding to C8.2 is compared with the %CO that corresponds with C8.1:



### 8.3.5 Output Weight Selection

In the previous subsection, better horizon selection remarkably improved the controlled variable with the highest output cost weight, namely the %CO. The relative pressure was neglected though, and it still remains positive for the entire duration of the simulation. This introduces a severe safety hazard, as discussed in the previous chapters. To improve the relative pressure regulation, its output cost weight should be increased relative to the other cost weights. Experiments show that the particular cost weight directly improves the relative pressure regulation when it is multiplied by a factor up to a maximum of ten. When it is multiplied by a factor larger than ten the improvement is not enough to justify the increase in cost weight. The controller settings are shown in Table 8.5. Fig.8.9 compares the relative pressure regulation with the settings of C8.3 to that of C8.2.



Table 8.5: Controller settings C8.3

Y(1)	Y(2)	Y(3)	U(1)	U(2)	M	P
4.5	1	0.036	400	400	2	6

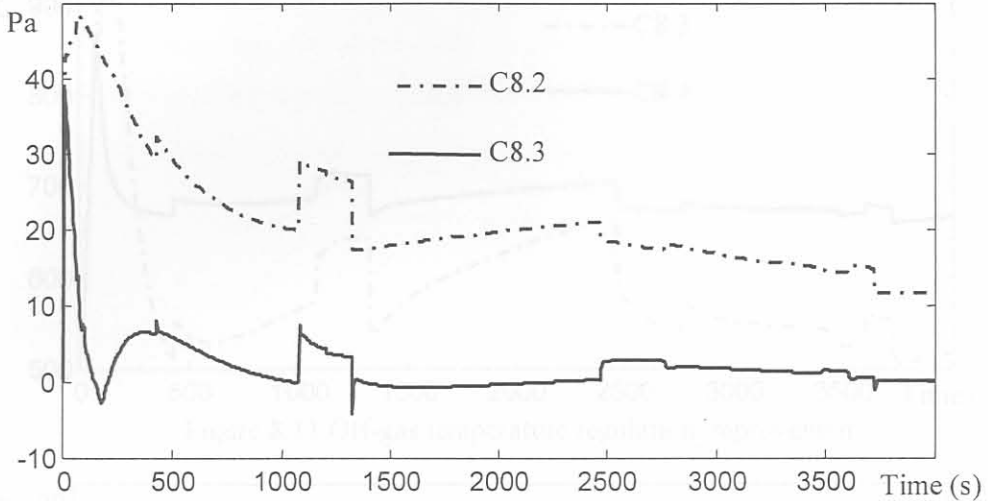


Figure 8.9 Relative pressure regulation improvement

Fig.8.10 shows the manipulated variables corresponding to C8.3.

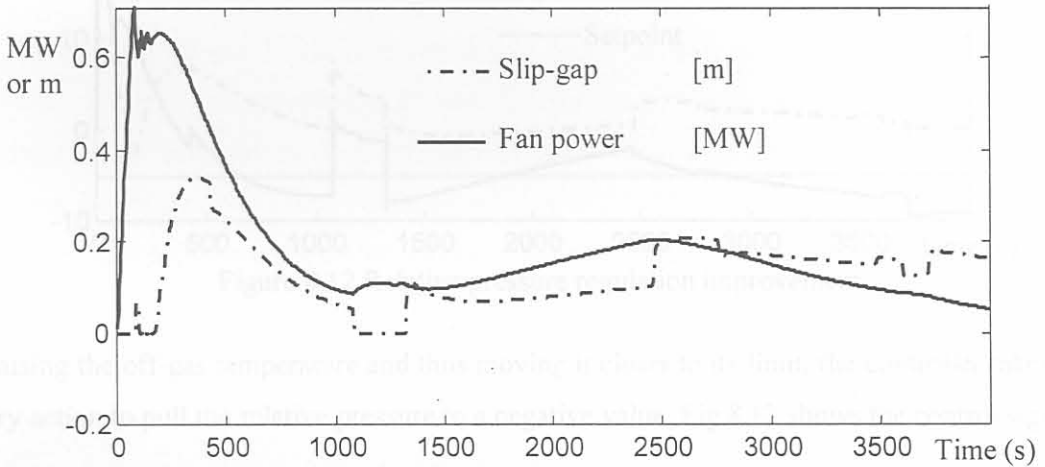


Figure 8.10 Control signals: Table 8.5: C8.3

The next adjustment made is to the output cost weight of the off-gas temperature. Experiments show that increase in the off-gas temperature cost weight brought the off-gas temperature closer to its limit and at the same time the relative pressure was made negative (setpoint = -5), although the regulation on the pressure was relaxed slightly. The off-gas temperature cost weight was multiplied by a factor of ten. A larger factor made the relative pressure too far negative and the off-gas %CO was also adversely affected. Table 8.6 indicates the new controller settings.

Table 8.6: Controller settings C8.4

Y(1)	Y(2)	Y(3)	U(1)	U(2)	M	P
4.5	1	<b>0.36</b>	400	400	2	6

Fig.8.11 compares the off-gas temperature between C8.4 and C8.3, while Fig.8.12 compares the relative pressure. It is clear from the figures that the emphasis shifted from regulating the pressure towards regulating the off-gas temperature (two conflicting agendas).

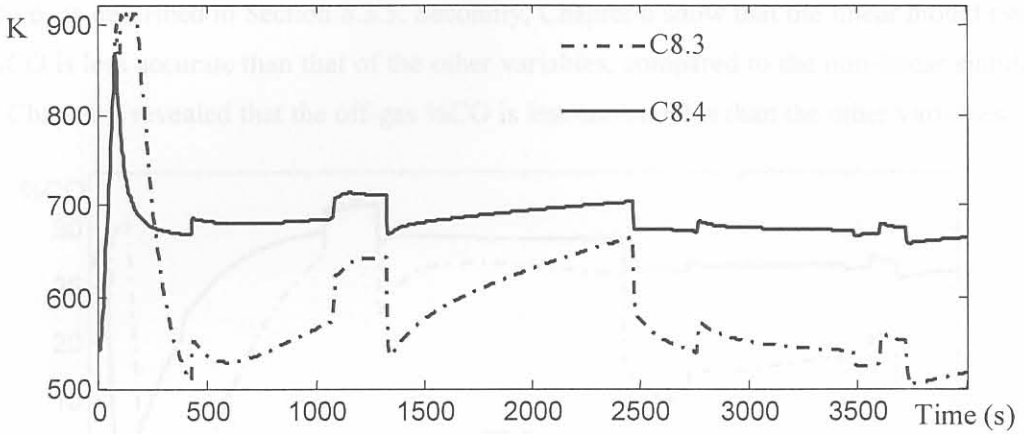


Figure 8.11 Off-gas temperature regulation improvement

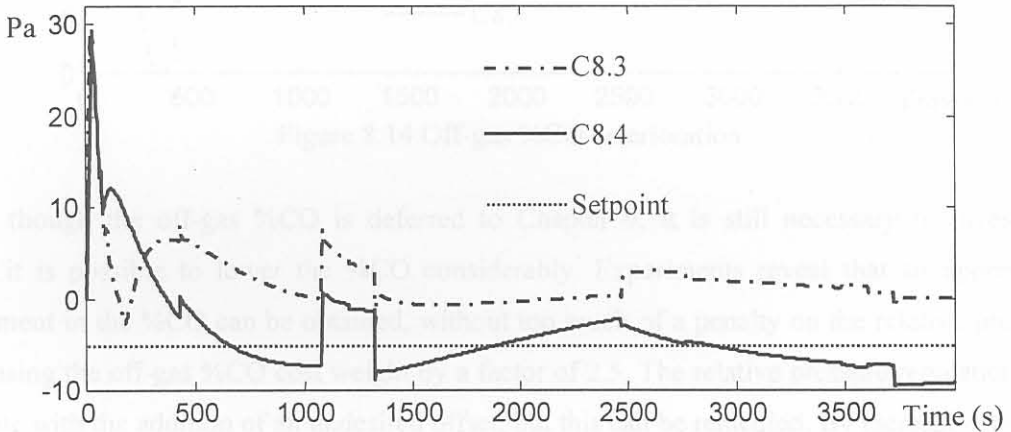


Figure 8.12 Relative pressure regulation improvement

By raising the off-gas temperature and thus moving it closer to its limit, the controller takes the necessary action to pull the relative pressure to a negative value. Fig.8.13 shows the control signals.

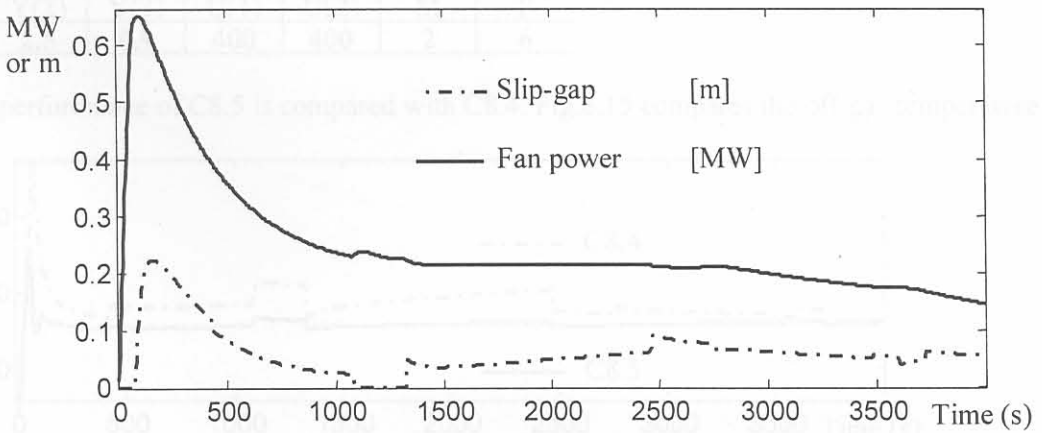


Figure 8.13 Control signals: Table 8.6: C8.4

As shown in Fig.8.14, this last controller tuning had a detrimental effect on the off-gas %CO, as it increases along with the off-gas temperature. There are three reasons why the off-gas %CO limit is not regarded as critically important here: Firstly, the off-gas %CO could not be brought below its limit before, as described in Section 8.3.5. Secondly, Chapter 6 show that the linear model estimate of the %CO is less accurate than that of the other variables, compared to the non-linear simulation. Thirdly, Chapter 7 revealed that the off-gas %CO is less controllable than the other variables.

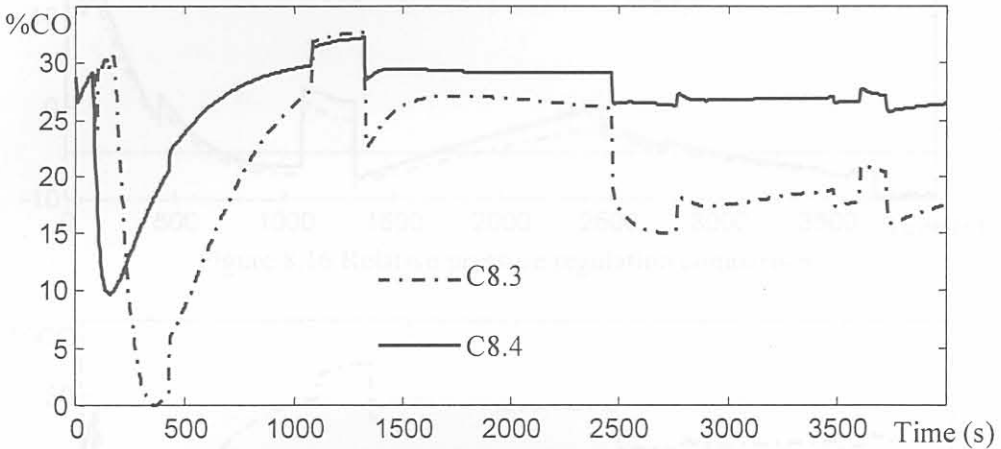


Figure 8.14 Off-gas %CO deterioration

Even though the off-gas %CO is deferred to Chapter 9, it is still necessary to investigate whether it is possible to lower the %CO considerably. Experiments reveal that an appreciable improvement in the %CO can be obtained, without too much of a penalty on the relative pressure, by increasing the off-gas %CO cost weight by a factor of 2.5. The relative pressure regulation does deteriorate with the addition of an undesired offset, but this can be remedied. By increasing the off-gas temperature cost weight by a factor of 2.5 as well, the pressure is brought back to its negative reference value. Table 8.7 summarises these controller settings.

Table 8.7: Controller settings C8.5

Y(1)	Y(2)	Y(3)	U(1)	U(2)	M	P
4.5	<b>2.5</b>	<b>0.9</b>	400	400	2	6

The performance of C8.5 is compared with C8.4. Fig.8.15 compares the off-gas temperature.

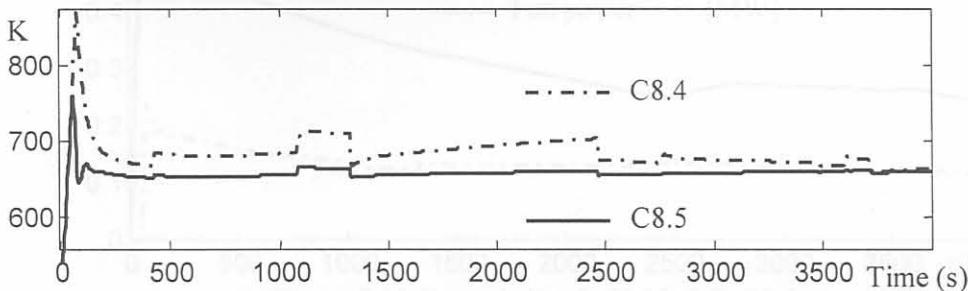


Figure 8.15 Off-gas temperature regulation comparison



Fig.8.16 compares the relative pressure regulation, which is slightly more relaxed for the final controller. Fig.8.17 compares the off-gas %CO, where the benefit of C8.5 is clearly seen.

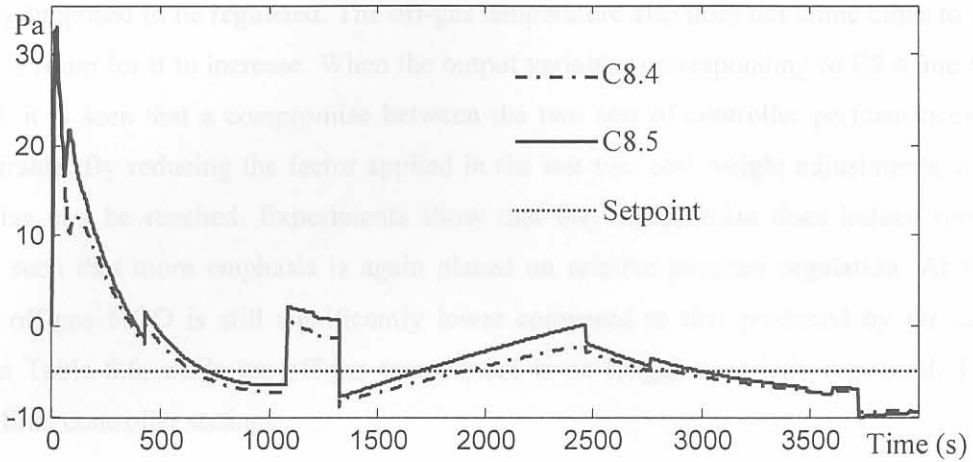


Figure 8.16 Relative pressure regulation comparison

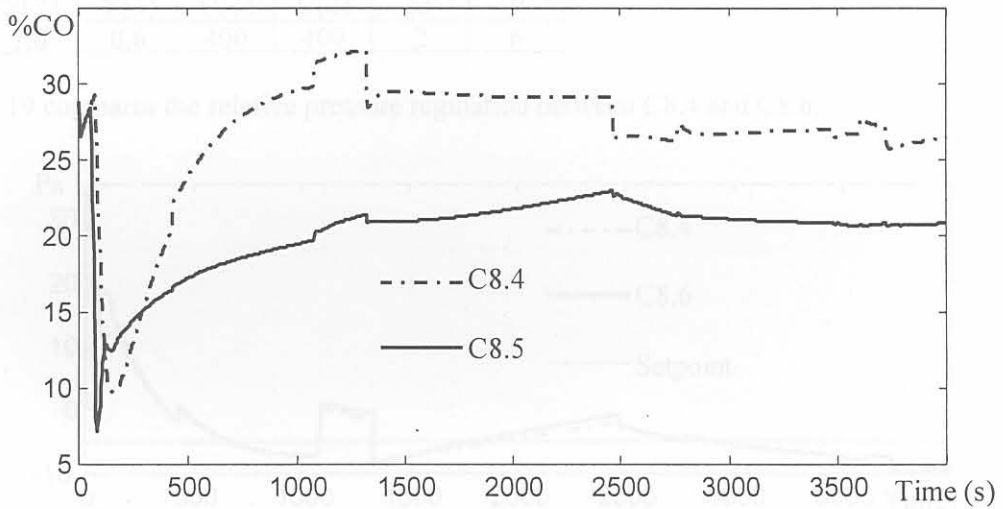


Figure 8.17 Off-gas %CO comparison

With C8.5 more emphasis is now placed on temperature regulation than on relative pressure regulation. Fig.8.18 shows the control signals corresponding to C8.5.

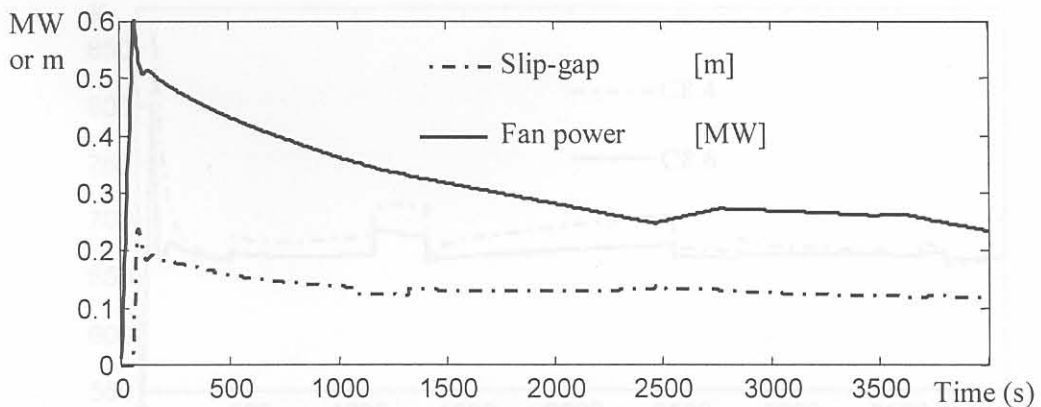


Figure 8.18 Control signals: Table 8.7: C8.5

The emphasis shift from relative pressure regulation to off-gas temperature regulation is undesirable. The off-gas temperature is not supposed to be regulated, only limited while the relative pressure is supposed to be regulated. The off-gas temperature also does not come close to its limit, and there is room for it to increase. When the output variables corresponding to C8.4, and C8.5 are compared, it is seen that a compromise between the two sets of controller performances will be more desirable. By reducing the factor applied in the last two cost weight adjustments, a suitable compromise can be reached. Experiments show that this compromise does indeed reverse the emphasis such that more emphasis is again placed on relative pressure regulation. At the same time, the off-gas %CO is still significantly lower compared to that produced by the controller settings in Table 8.6, while the off-gas temperature is no longer as strictly regulated. Table 8.8 gives the final controller settings.

Table 8.8: Final controller settings C8.6

Y(1)	Y(2)	Y(3)	U(1)	U(2)	M	P
4.5	<b>1.6</b>	<b>0.6</b>	400	400	2	6

Fig.8.19 compares the relative pressure regulation between C8.4 and C8.6.

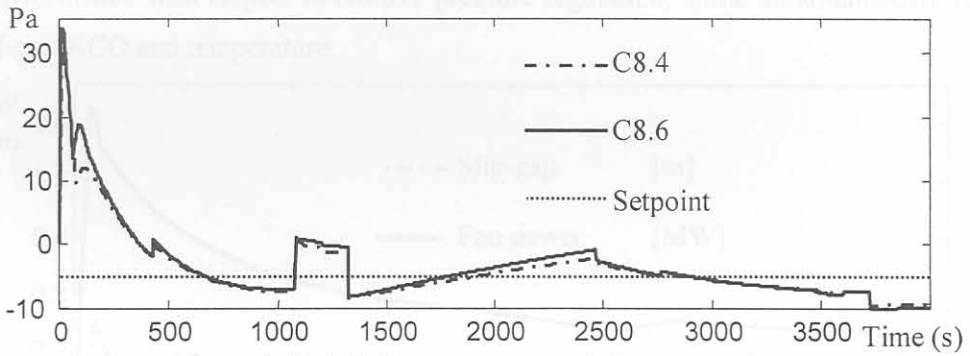


Figure 8.19 Relative pressure regulation comparison

Fig.8.20 compares the off-gas temperature produced by C8.4 and C8.6.

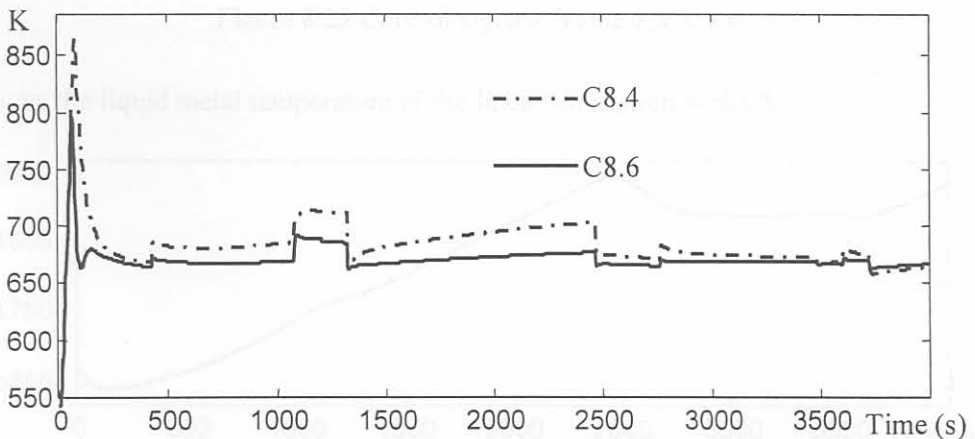


Figure 8.20 Off-gas temperature regulation comparison

Fig.8.21 compares the off-gas %CO produced by C8.4 and C8.6.

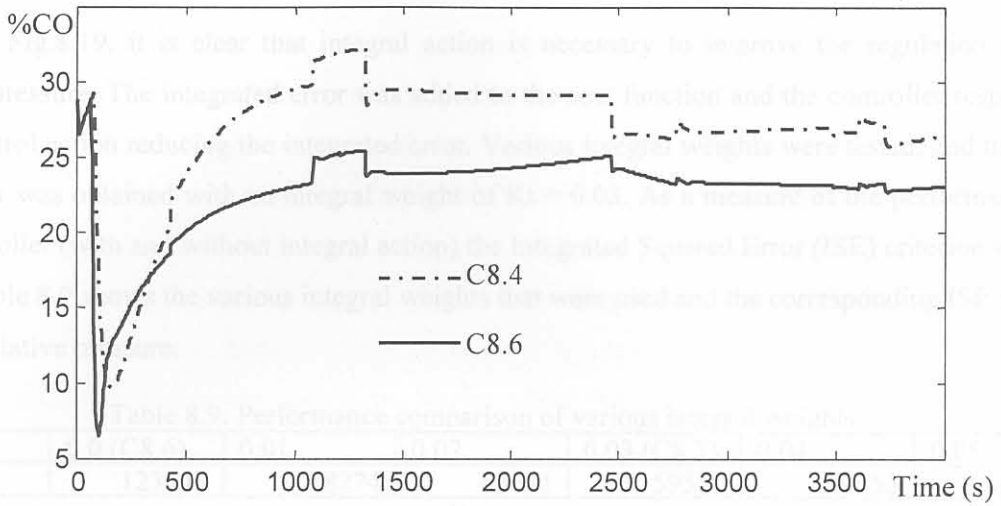


Figure 8.21 Off-gas %CO comparison

Fig.8.22 shows the control signals of the final controller. It is evident that the compromise results in smoother control actions and at the same time strengthening them against the effects of unmeasured disturbances. The final controller settings enable the controller to maintain practically the same performance with respect to relative pressure regulation, while simultaneously reducing both the off-gas %CO and temperature.

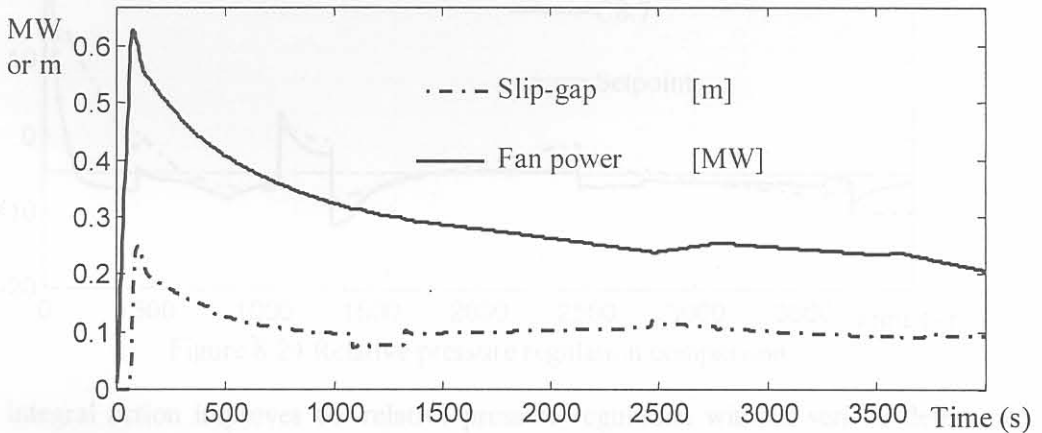


Figure 8.22 Control signals: Table 8.8: C8.6

Fig.8.23 shows the liquid metal temperature of the linear simulation with C8.6.

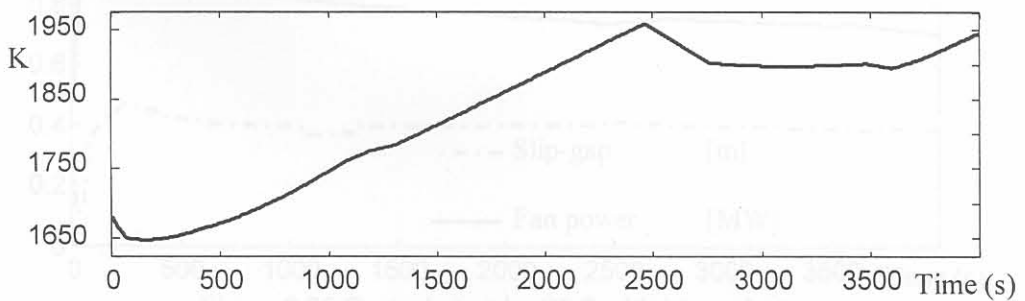


Figure 8.23 Liquid metal temperature: C8.6



### 8.4 INTEGRAL ACTION

From Fig.8.19, it is clear that integral action is necessary to improve the regulation of the relative pressure. The integrated error was added to the cost function and the controller responded with control action reducing the integrated error. Various integral weights were tested, and the best controller was obtained with an integral weight of  $K_i = 0.03$ . As a measure of the performance of the controller (with and without integral action) the Integrated Squared Error (ISE) criterion will be used. Table 8.9 shows the various integral weights that were used and the corresponding ISE values for the relative pressure.

Table 8.9: Performance comparison of various integral weights

Weight	0.0 (C8.6)	0.01	0.02	0.03 (C8.7)	0.04	0.05
ISE	123449	78274	63611	59557	59753	60301

In Fig.8.24 the performance of the controller with integral action (C8.7) on relative pressure is compared to that of the controller without integral action (C8.6):

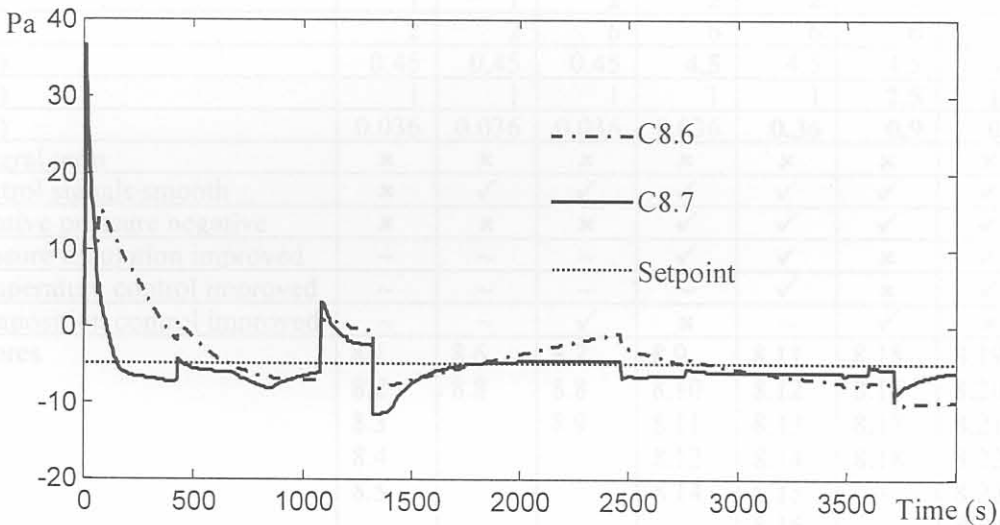


Figure 8.24 Relative pressure regulation comparison

The integral action improves the relative pressure regulation without serious deterioration of either of the other two outputs. Fig.8.25 shows the control signals corresponding to C8.7:

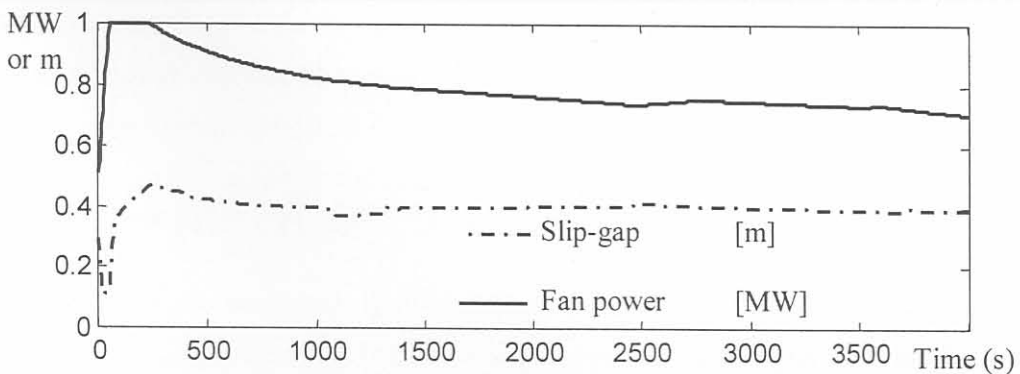


Figure 8.25 Control signals: C8.7 with integral

## 8.5 CONCLUSION

The controller was designed by selecting the various parameters that are available for design. By increasing the input cost function weights, the control signal noise was reduced. By increasing the manipulation horizon (M) and the prediction horizon (P), the range over which optimisation is done is increased, thus improving the controller's ability to select the optimal MVs. Selecting the output cost function weights achieves the necessary emphasis shifts. The use of an integral term in the cost function enables the controller to eliminate unwanted offsets, and therefore improves the setpoint tracking and regulation. Table 8.10 gives a summary of the various controllers in this chapter, indicating characteristics and the figures where the corresponding inputs or outputs are shown:

Table 8.10 Summary of control characteristics

	C8.0	C8.1	C8.2	C8.3	C8.4	C8.5	C8.6	C8.7
U(1)&U(2)	1	<b>400</b>	400	400	400	400	400	400
M	1	1	<b>2</b>	2	2	2	2	2
P	2	2	<b>6</b>	6	6	6	6	6
Y(1)	0.45	0.45	0.45	<b>4.5</b>	4.5	4.5	4.5	4.5
Y(2)	1	1	1	1	1	<b>2.5</b>	<b>1.6</b>	1.6
Y(3)	0.036	0.036	0.036	0.036	<b>0.36</b>	<b>0.9</b>	<b>0.6</b>	0.6
Integral term	x	x	x	x	x	x	x	✓
Control signals smooth	x	✓	✓	✓	✓	✓	✓	✓
Relative pressure negative	x	x	x	✓	✓	✓	✓	✓
Pressure regulation improved	~	~	~	✓	✓	x	✓	✓
Temperature control improved	~	~	~	~	✓	x	✓	~
Composition control improved	~	~	✓	x	~	✓	x	~
Figures	8.1	8.6	8.7	8.9	8.11	8.15	8.19	8.24
	8.2	8.8	8.8	8.10	8.12	8.16	8.20	8.25
	8.3		8.9	8.11	8.13	8.17	8.21	
	8.4			8.12	8.14	8.18	8.22	
	8.5			8.14	8.15		8.23	
					8.16		8.24	
					8.17			
					8.19			
					8.20			
					8.21			

## 9.2 SIMULATION STRUCTURE

The structure of the simulation is illustrated in the program flowchart in Fig 9.1, where the blocks with both edges indicate algorithms that are discussed in more detail. The disturbance model and actual conditions are the same as those discussed in Chapter 5. The internal model is defined by